Ultrasound-assisted one-pot multi-component synthesis of 2-pyrrolidinon-3-olates catalyzed by Co$_3$O$_4$@SiO$_2$ core–shell nanocomposite

Mohammad Ali Ghasemzadeh & Mohammad Hossein Abdollahi-Basir

Taylor & Francis
Taylor & Francis Group

Ultrasound-assisted one-pot multi-component synthesis of 2-pyrrolidinon-3-olates catalyzed by Co$_3$O$_4$@SiO$_2$ core–shell nanocomposite

Mohammad Ali Ghasemzadeh and Mohammad Hossein Abdollahi-Basir

Department of Chemistry, Qom Branch, Islamic Azad University, Qom, Iran

ABSTRACT

2-pyrrolidinon-3-olates were synthesized via one-pot four-component reaction of 2-aminobenzothiazole, aromatic aldehydes, dimethyl acetylenedicarboxylate and morpholine/piperidine in the presence of Co$_3$O$_4$@SiO$_2$ core–shell nanocomposite as catalyst under ultrasound irradiation. The protocol offers several such advantages as high yields, short reaction time and mild reaction conditions with reusability of the catalyst. The core–shell nanocomposite was also prepared using ultrasound irradiation and the structure and magnetic properties were fully characterized by TEM, FE-SEM, XRD, EDX, FT-IR and VSM analysis.
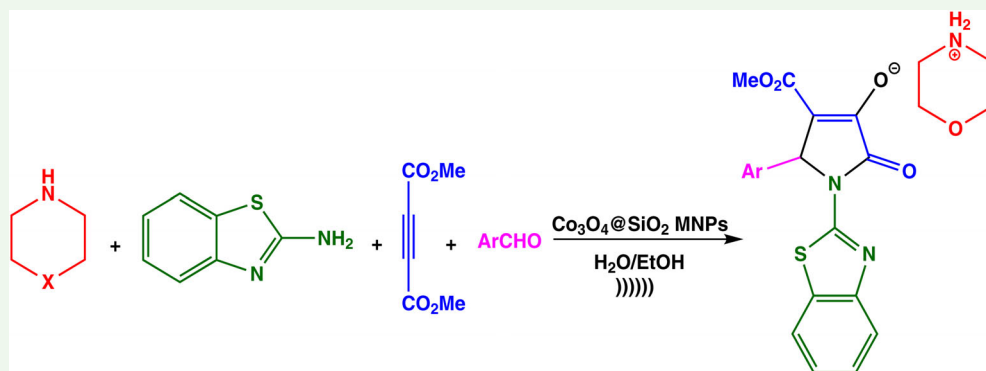
Introduction

Multi-component reactions (MCRs) are significant in producing a great level of diversity, as they allow more than two building units to be combined with practical synthesis. Furthermore, MCRs are easy to perform, inexpensive, quick, energy efficient and experimental procedures are relatively simple (1). Recently, the application of ultrasonic irradiation in chemical syntheses has received much attention (2–5). On the other hand, designing MCRs under ultrasonic irradiation is another attractive area in synthetic organic chemistry. The ultrasound irradiation technique is especially useful in the chemistry process which requires drastic conditions or prolonged reaction time (6). The advantages of this technique in organic transformation are simple experimental procedure, environmental friendliness, good yields and short reaction time.

Ultrasound accelerated chemical reactions are well known and to be proceeded via the formation and adiabatic collapse of transient cavitations bubbles. In addition, ultrasound irradiation has been demonstrated as an alternative energy source for organic reactions ordinarily accomplished by heating. Many homogeneous and heterogeneous reactions can be smoothly conducted by sonication to improve the reaction yield.

2-Pyrrolidinone derivatives have shown significant biological and pharmacological activities which can be applied in drugs, especially to cure neurological disorders, such as seizures, Alzheimer's, senile dementia and concussion (7). The 2-pyrrolidinone template is also considered as an essential pharmacophore group
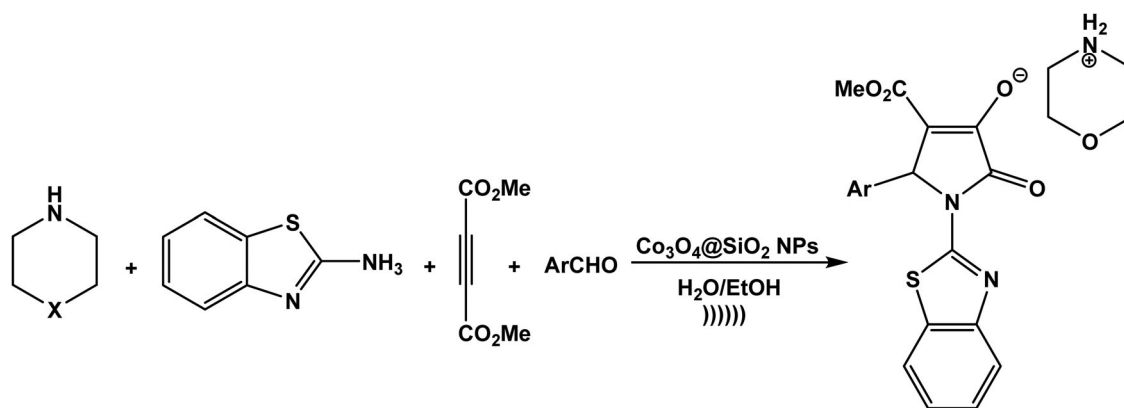
Scheme 1. Synthesis of 2-pyrrolidinon-3-olates in the presence of $Co_3O_4@SiO_2$ nanocomposites under sonication conditions.

which has aggregation-inhibiting effects (*8*). Moreover, it has been shown that the 2-pyrrolidinone-based chemical structures have some anticonvulsant and pharmacological activities (*9*), including a modulator in those H_3 receptors associated with the central nervous system (*10*).

From both academic and industrial points of view, the development of efficient and practical catalysts for organic synthesis is of considerable interest (*11*). In recent years, tremendous interest has been devoted to perform various chemical transformations under heterogeneous conditions owing to simplicity in operation, remarkable recyclability and its eco-friendly nature (*12*).

During recent decades, nanometal oxides have attracted extensive attention in various catalytic processes due to their unique properties; these high reactivities are due to high surface areas combined with unusually reactive morphologies (*13*). Coating metal nanoparticles with an amorphous silica layer is a promising and significant approach in the expansion of nanoparticles for both basic study and technological applications. Silica surfaces are chemically inert, biocompatible and can be easily functionalized for conjugation target. Therefore, the outer shell of silica not only protects the inner magnetite core from oxidation, but also provides sites for surface functionalization using various groups (*14*).

In the recent years, core–shell nanostructures were used as an efficient catalytic systems in many MCRs, such as synthesis of diazepine derivatives (*15*), indazolo[2,1-b]phthalazine-triones and pyrazolo[1,2-b]phthalazine-diones (*16*), 3,4-dihydropyrimidin-2(1H)-ones (*17*), 1,8-dioxo-octahydroxanthenes (*18*), quinoxaline derivatives (*19*) and 1,4-dihydropyridines (*20*).

In this regard, $Co_3O_4@SiO_2$ nanocomposite has been found to possess unique characteristics, such as environmental compatibility, non-toxicity, reusability and non-corrosively. Furthermore, this kind of nanostructures showed both chemical and physical stability over a prolonged duration of time.

In spite of importance of 2-pyrrolidinon-3-olates, there is only one report in the case of synthesis of these compounds (*21*) with long reaction time (two days) and moderate yields. Therefore, the significant role of these compounds as biologic heterocyclic compounds prompted us to improve the pathway to the synthesis of these molecules using ultrasound irradiation.

In continuation to improve the synthetic approach for the production of various medicinally active compounds using reusable nanocatalysts and ultrasonic irradiation (*22–26*), herein we combined the advantages of ultrasonic irradiation and nanotechnology to design a new
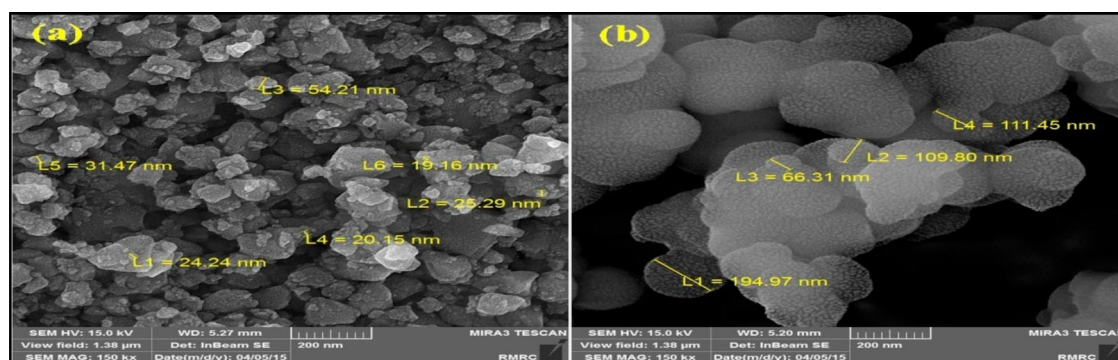
Figure 1. FE-SEM images of Co_3O_4 NPs (a) and $Co_3O_4@SiO_2$ (b) nanocomposites.
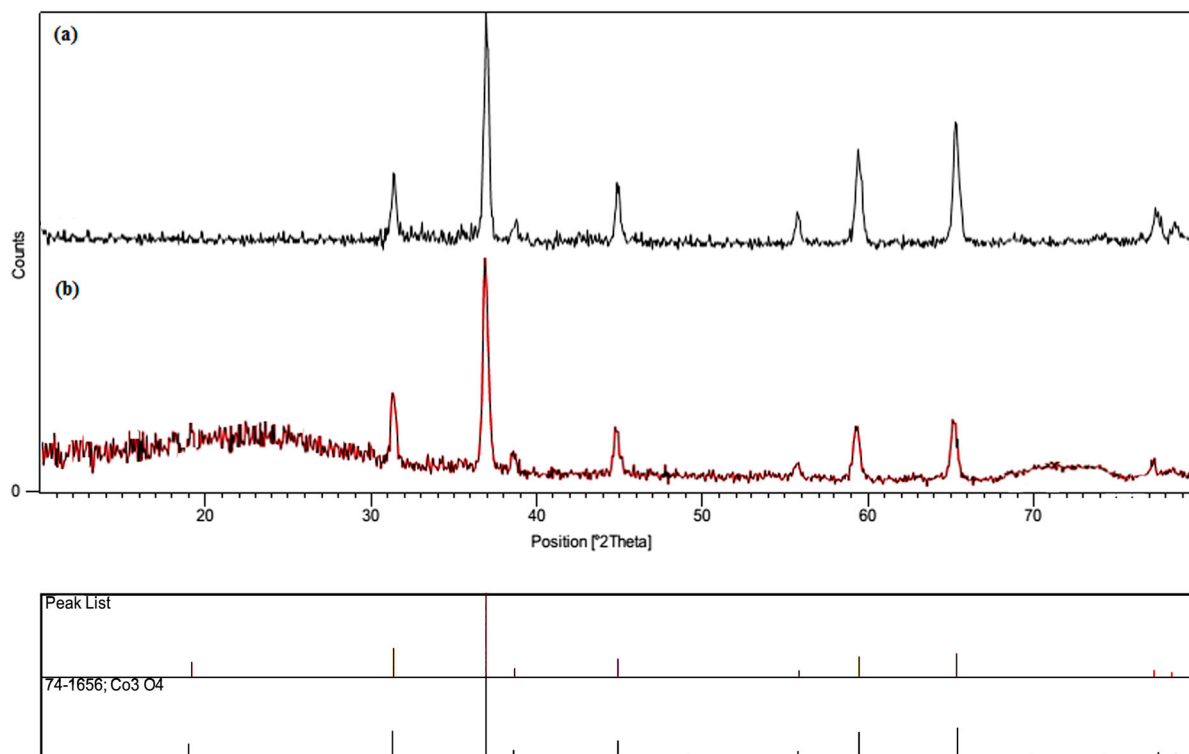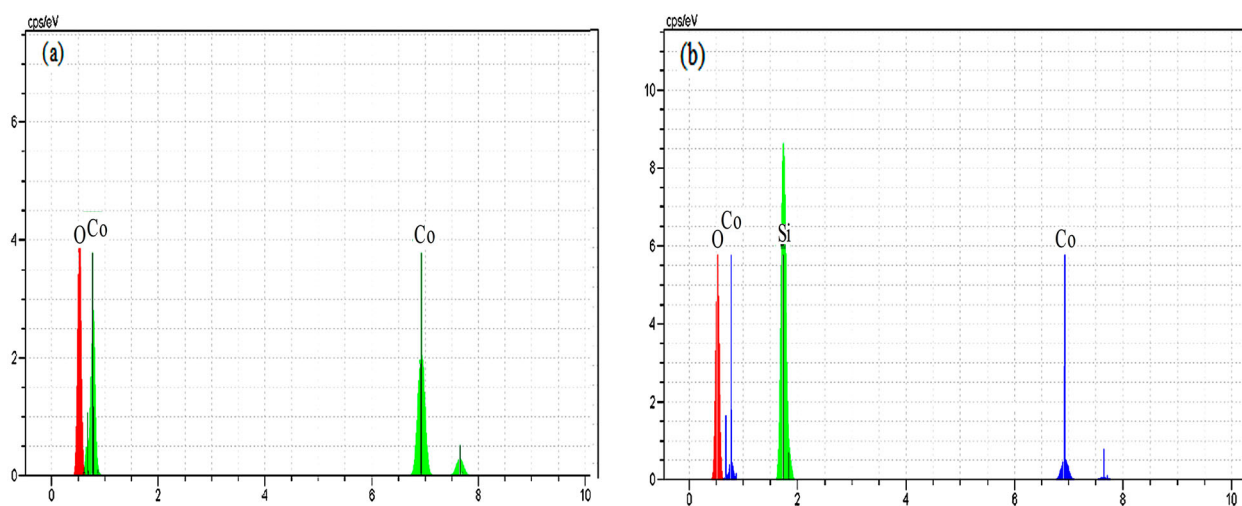
Figure 2. X-ray diffraction of Co_3O_4 NPs (a) and $Co_3O_4@SiO_2$ (b) nanocomposites.

and efficient method for synthesis of 2-pyrrolidinon-3-olate derivatives using $Co_3O_4@SiO_2$ nanocomposites as an efficient and reusable heterogeneous catalyst under ultrasonic irradiation (Scheme 1).

Results and discussion

The morphology and structure of the nanocatalyst before and after silica coating were studied by scanning electron microscopy (FE-SEM) (Figure 1). The SEM observations

indicate that the Co_3O_4 nanoparticles have an average diameter ranging about 25–30 nm (Figure 1(a)). The silica-modification process of nanoparticles leads to the formation of cobalt/silica nanocomposites with typical core–shell structure. These observations confirmed the formation of a silica layer around the Co_3O_4 NPs. Figure 1(b) indicates that the $Co_3O_4@SiO_2$ nanocomposites still keep the morphological properties of Co_3O_4 except for a slightly larger particle size and smoother surface.

Figure 3. EDX spectra of Co_3O_4 NPs (a) and $Co_3O_4@SiO_2$ (b) nanocomposites.
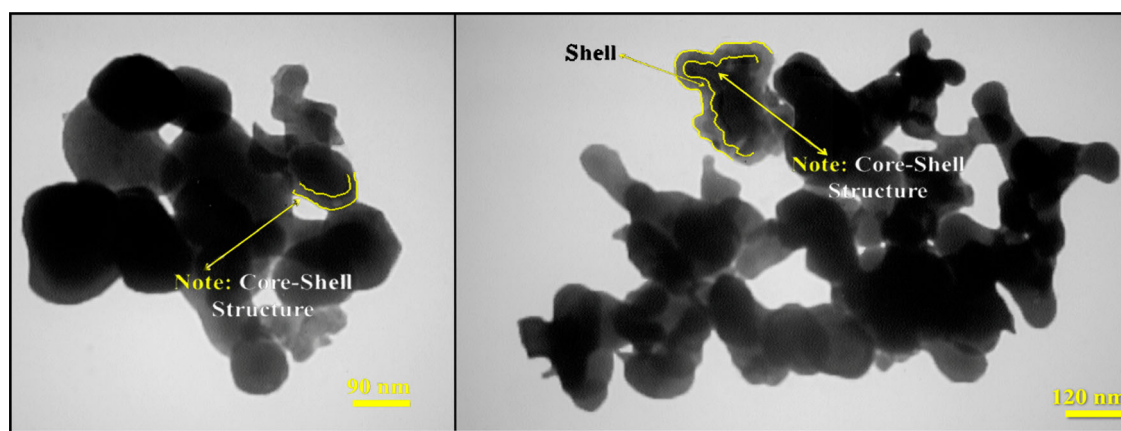
Figure 4. TEM images of Co$_3$O$_4$@SiO$_2$ nanocomposites.

The X-ray diffraction (XRD) patterns of Co$_3$O$_4$ and Co$_3$O$_4$@SiO$_2$ nanostructures are shown in Figure 2. The XRD pattern of Co$_3$O$_4$ shows reflections at 19.09, 31.26, 36.89, 38.47, 44.77, 59.19, 65.27, 74.26 and 78.80 corresponding to (111), (220), (311), (222), (400), (511), (440), (620) and (622) planes of cubic normal spinel Co$_3$O$_4$ (JCPDS No. 74–1656).

As can be seen, the position and relative intensities of all peaks are compatible with the standard XRD pattern of Co$_3$O$_4$ (27). Moreover, The XRD pattern of Co$_3$O$_4$@SiO$_2$ nanocomposites exhibited similar diffraction peaks to that of the Co$_3$O$_4$ NPs, indicating that the cobalt phase was also present in the form of Co$_3$O$_4$ cubic spinel structure during functionalization (Figure 2(b)). The amorphous silica (SiO$_2$) coating of Co$_3$O$_4$ by the presence of the new broad peak at 2θ approximately 22–25°.

The chemical purity of the samples as well as their stoichiometry was tested by EDX studies. The EDX spectrum given in Figure 3(a) shows the presence of Co and O

as the only elementary components of Co$_3$O$_4$ NPs. Also, the EDX spectrum of Co$_3$O$_4$@SiO$_2$ shows the elemental compositions of the core–shell nanocomposites, which contains Co, O and Si (Figure 3(b)).

The size and morphology of Co$_3$O$_4$@SiO$_2$ nanocomposites were analyzed by transmission electron microscopy (TEM) (Figure 4). The results show that these nanocatalysts consist of spherical particles with the crystallite size about 60–70 nm, which is in good agreement with the results obtained from the scanning electron microscopy images.

The FT-IR spectra of Co$_3$O$_4$ nanoparticles and Co$_3$O$_4$@SiO$_2$ nanocomposite are shown in Figure 5. For the bare Co$_3$O$_4$ nanoparticles (Figure 5(a)), the vibration bands at 565 and 662 cm^{-1} are the typical IR absorbance induced by structure Co-O vibration. In the case of the Co$_3$O$_4$@SiO$_2$ nanocomposite (Figure 5(b)), the band at 1070 cm^{-1} is corresponding to Si-O-Si antisymmetric stretching vibrations, being indicative of the existence of SiO$_2$ on the nanoparticles.
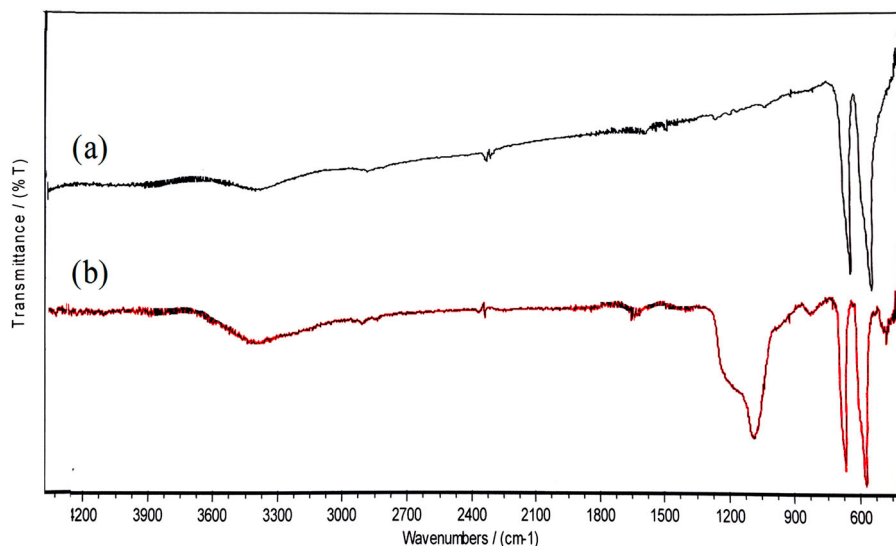
Figure 5. Comparative FT-IR spectra of Co$_3$O$_4$ NPs (a) and Co$_3$O$_4$@SiO$_2$ (b).
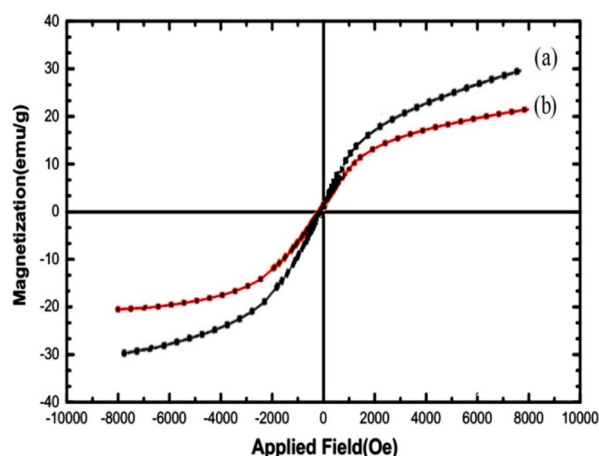
Figure 6. VSM magnetization curves of the Co_3O_4 NPs (a) and $Co_3O_4@SiO_2$ (b).

The magnetic properties of the uncoated Co_3O_4 and $Co_3O_4@SiO_2$ were measured by a vibrating sample magnetometer (VSM), at room temperature (Figure 6). The hysteresis loops which are characteristic of super paramagnetic behavior can be clearly observed for all the nanostructures. Superparamagnetism is the responsiveness to an applied magnetic field without retaining any magnetism after removal of the applied magnetic field. From M versus H curves, the saturation magnetization value (Ms) of uncoated Co_3O_4 NPs was found to be 32.22 emu g^{-1}. However, the magnetization obtained for the $Co_3O_4@SiO_2$ in the same field was 21.98 emu g^{-1} being lower than that of the uncoated Co_3O_4. These results indicated that the magnetization of Co_3O_4 decreased considerably with coating the silica shell. This is mainly attributed to the existence of nonmagnetic materials on the surface of the nanoparticles.

In this research, in order to determine the optimum reaction conditions and investigate the ultrasonic effect, four-component condensation of 2-aminobenzothiazole (1 mmol), dimethyl acetylenedicarboxylate

(1 mmol), benzaldehyde (1 mmol) and morpholine (1 mmol) in aqueous ethanol media was selected as a model reaction (Scheme 2).

In order to study the effect of various catalysts under ultrasonic irradiation, catalytic behaviors of six types of catalysts such as MgO, Fe_3O_4, p-TSA, CuI, Mn_3O_4 and $Co_3O_4@SiO_2$ were investigated on the model reaction (Table 1). The results showed that compound 5a provided high yield within short reaction time in the presence of the $Co_3O_4@SiO_2$ nanocomposites. As shown in Table 1, the product yield was found to be traced in the absence of a catalyst.

Furthermore, in order to show the merit of the present work toward the previous study (21), the model reaction was carried out to compare the results with previous conditions (Table 1, entry 5).

To find the optimum amount of the catalyst, the preparation of 2-pyrrolidinon-3-olate (5a) was carried out using different amounts of $Co_3O_4@SiO_2$ as the catalyst (0.001, 0.003, 0.005, 0.01 g). The best result was obtained

Table 1. Optimization of the model reaction using various catalysts.[a]

Entry	Catalyst	Time	Yield (%)[b]
1	None	70 min	Trace
2	MgO NPs	60 min	42
3	Fe_3O_4 NPs	43 min	60
4	p-TSA	47 min	72
5	p-TSA	2 days[c]	62[21]
6	CuI NPs	40 min	65
7	Mn_3O_4 NPs	45 min	75
8	SiO_2 NPS	40 min	70
9	$Co_3O_4@SiO_2$ NPs	30 min	96

[a]Reaction conditions: 2-aminobenzothiazole, dimethyl acetylenedicarboxylate, benzaldehyde and morpholine (1:1:1:1 molar ratio) in aqueous ethanol media using 0.01 g of each catalyst at room temperature under ultrasonication.
[b]Isolated yields.
[c]Reaction conditions: 2-aminobenzothiazole, dimethyl acetylenedicarboxylate, benzaldehyde and morpholine (1:1:1:1 molar ratio) in ethanol (10 mL) using 0.25 mmol of p-TSA at 55°C.
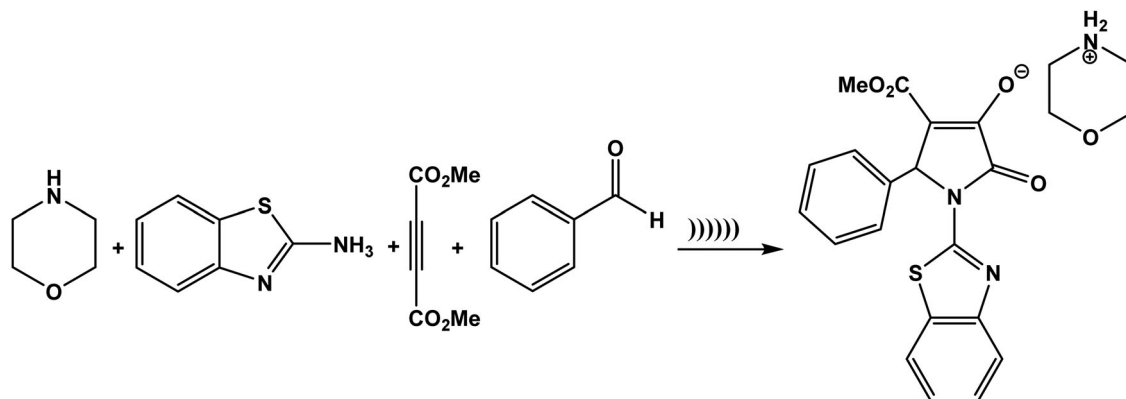
Scheme 2. The model reaction for the synthesis of 2-pyrrolidinon-3-olate (5a).

Table 2. Optimization of the model reaction using various solvents.[a]

Entry	Solvent	Time (min)	Yield (%)[b]
1	Solvent free (r.t.)	60	Trace
2	DMF	50	65
3	H_2O	45	55
4	CH_3CN	35	70
5	$PhCH_3$	60	40
6	CH_2Cl_2	55	45
7	Ethanol	40	84
8	$H_2O/EtOH$ (1:1)	30	96
9	$H_2O/EtOH$ (1:1)	2 days[c]	82

[a]Reaction conditions: 2-aminobenzothiazole, dimethyl acetylenedicarboxylate, benzaldehyde and morpholine (1:1:1:1 molar ratio) using 0.003 g of $Co_3O_4@SiO_2$ under ultrasonication.
[b]Isolated yields.
[c]Reaction conditions: 2-aminobenzothiazole, dimethyl acetylenedicarboxylate, benzaldehyde and morpholine (1:1:1:1 molar ratio) in water/EtOH (10 mL) at 55°C.

by using 0.003 g of the $Co_3O_4@SiO_2$ nanostructures under ultrasound irradiation.

Selection of suitable solvent is a crucial issue for a successful ultrasound-assisted synthesis. The influence of solvent on the model reaction was studied using the $Co_3O_4@SiO_2$ nanocomposites in the various solvents as well as solvent-free conditions (Table 2). As shown in Table 2 the results remarkably depend on the nature of the solvent. The best result (96% yield, 30 min) was obtained in water–ethanol at room temperature for the multi-component synthesis of 2-pyrrolidinon-3-olates (5a) under sonication (Table 2, entry 8). Hence, water–ethanol was used as the best solvent for all the further reactions. It seems that the remarkable differences between the results presented in Table 2 are related to the hydrogen bonding between water–ethanol and substrates which promote the nucleophilic attack of the reactants.

To compare the sonication effect and the conventional heating in the synthesis of 2-pyrrolidinon-3-olates, the four-component reactions of 2-aminobenzothiazole, aldehydes, dimethyl acetylenedicarboxylate and morpholine/piperidine were conducted under both ultrasound and conventional heating conditions in the presence of $Co_3O_4@SiO_2$ nanocomposite. According to Table 3, ultrasound irradiation had significant influence and increased product yields within shorter reaction times. Moreover, it can be observed that ultrasound irradiation was found to have astonishing effect on the synthesis of 2-pyrrolidinon-3-olates 5a–k since the reaction time decreased to less than 40 minutes compared to 48 h in conventional procedure. Also, the reaction yields were significantly improved by 10–25% under the ultrasonic irradiation condition.

According to Table 3, the aryl aldehydes with electron-withdrawing groups, such as NO_2 and Cl, in *p*-position reacted with 2-aminobenzothiazole, dimethyl acetylene-dicarboxylate and morpholine/piperidine very smoothly, while the reactants with electron-donating groups, such as hydroxy and methoxy, proceeded with the longer reaction time along with the lower product yields. In addition, the sterically hindered aldehydes reacted more slowly in comparison with the unhindered ones.

Proposed mechanism

A plausible mechanism for the synthesis of pyrrolidinon-3-olate derivatives using $Co_3O_4@SiO_2$ nanocomposites has been shown in Scheme 3, based on the previous study (21). In general, the $Co_3O_4@SiO_2$ can act as a Lewis acid in order to increase the electrophilicity of the carbonyl group of the aldehydes and intermediates. Moreover, the nanocomposite is able to coordinate with the unsaturated C=C bonds of the reactants. First, the condensation between morpholine/piperidine and

Table 3. Synthesis of pyrrolidinon-3-olate derivatives under ultrasonic irradiation and conventional method.[a]

Entry	Ar	X	Product	Conventional method[b] Time (h)	Yield (%)[d]	Ultrasound irradiation[c] Time (min)	Yield (%)[d]	m.p. (°C)	Lit. m.p. (°C)
1	C_6H_5	O	5a	48	82	30	96	218–220	221.3–221.61[21]
2	4-MeO-C_6H_4	O	5b	48	73	38	90	194–195	192.1–192.5[21]
3	4-CH(CH$_3$)$_2$-C_6H_4	O	5c	48	71	40	88	196–197	196.2–196.5[21]
4	4-Me-C_6H_4	O	5d	48	74	36	90	218–219	218.3–218.7[21]
5	3-NO$_2$-C_6H_4	O	5e	48	77	28	93	194–196	197.7–197.9 [21]
6	4-Me-C_6H_4	CH$_2$	5f	48	72	34	91	201–203	198–200[21]
7	3-Me-C_6H_4	CH$_2$	5g	48	78	32	93	209–211	210–212 [21]
8	4-NO$_2$-C_6H_4	O	5h	48	81	23	97	198–199[e]	–
9	4-Cl-C_6H_4	O	5i	48	83	23	97	192–194[e]	–
10	4-Br-C_6H_4	O	5j	48	81	25	95	176–178[e]	–
11	4-OH-C_6H_4	O	5k	48	63	40	88	209–211[e]	–

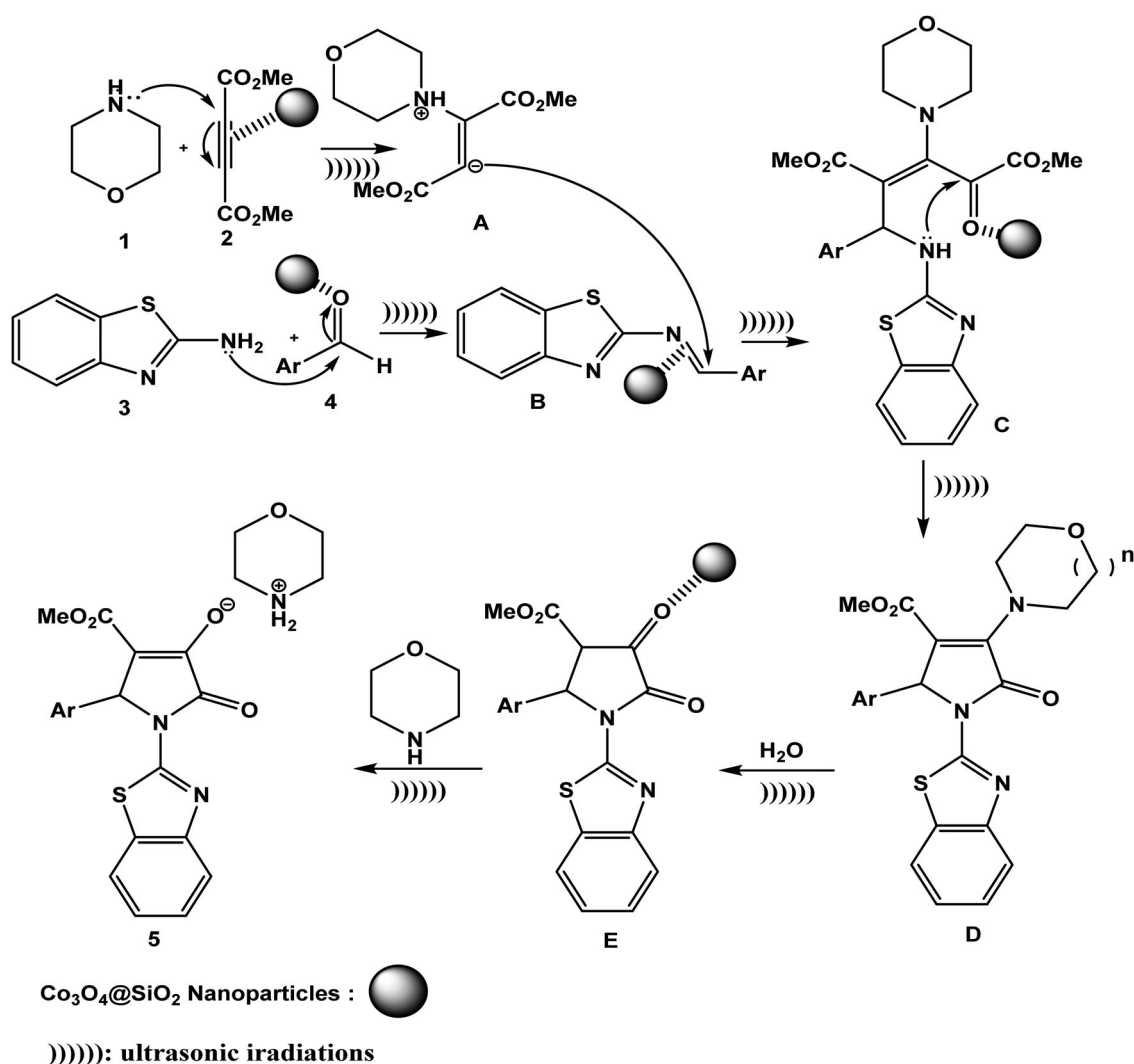[a]Reaction conditions: 2-aminobenzothiazole, dimethyl acetylenedicarboxylate, aldehyde and morpholine/piperidine (1:1:1:1 molar ratio) using 0.003 g of $Co_3O_4@SiO_2$.
[b]Stirring condition in $H_2O/EtOH$ ((1:1),10.0 mL), at r.t. 20 min., and then at 50–60°C for 48 h.
[c]Under ultrasonic waves (power intensity: 40%) in $H_2O/EtOH$ ((1:1),10.0 mL), at 25°C.
[d]Isolated yields.
[e]New compounds.

Scheme 3. The proposed mechanism for the synthesis of pyrrolidinon-3-olate derivatives catalyzed by $Co_3O_4@SiO_2$.

dimethyl acethylenedicatboxylate is suggested to give intermediate A. Then the nucleophilic attack of 2-amino-benzothiazole to aldehyde leads to the formation of intermediate B. Afterwards, a Michael addition reaction took place between intermediates A and B in order to form intermediate C, followed by the intramolecular cyclization to obtain intermediate D catalyzed by the $Co_3O_4@SiO_2$ core–shell nanocomposites. In the last step, the hydrolysis of intermediate D produces intermediate E, which is reacted to morpholine/piperidine to produce the final product 5.

Experimental

Chemicals were purchased from the Sigma-Aldrich and Merck in high purity. All of the materials were of commercial reagent grade and were used without further purification. All melting points are uncorrected and

were determined in capillary tube on a Boetius melting point microscope. The ultrasonic irradiation was used in the reactions by a multi-wave ultrasonic generator (Sonicator 3200; Bandelin, MS 73, Germany), equipped with a converter/transducer and titanium oscillator (horn), 12.5 mm in diameter, operating at 20 kHz with a maximum power output of 200 W. The ultrasonic generator automatically adjusted the power level. ^1H NMR and ^{13}C NMR spectra were obtained on Bruker 400 MHz spectrometer with $CDCl_3$ as the solvent using TMS as an internal standard. FT-IR spectrum was recorded on a Magna-IR, spectrometer 550. The elemental analyses (C, H, N) were obtained from a Carlo ERBA Model EA 1108 analyzer. Powder XRD was carried out on a Philips diffractometer of X'pert Company with mono chromatized Cu Kα radiation (λ = 1.5406 Å). Microscopic morphology of products was visualized by SEM (LEO 1455VP). The mass spectra were recorded on a

Joel D-30 instrument at an ionization potential of 70 eV. TEM was performed with a Jeol JEM-2100UHR, operated at 200 kV. Magnetic properties were obtained on a BHV-55 VSM made by MDK-I. R. Iran. The compositional analysis was done by energy-dispersive analysis of X-ray (EDX, Kevex, Delta Class I).

Preparation of Co_3O_4 nanoparticles

Co_3O_4 nanoparticles were prepared according to the previously reported procedure by Vela et al. with some modifications (28).

First, cobalt nitrate hexahydrate (8.60 g) was dissolved in 100 mL of ethanol and the mixture was vigorously stirred. Then, the mixture was heated to 50°C and kept for 30 min. Finally, oxalic acid (2.14 g) was added quickly to the solution and the reaction mixture was stirred for 2 h at 50°C. The formed precipitate including cobalt (II) oxalate was collected by centrifuge, followed by calcination at 400°C for 2 h to produce the Co_3O_4 nanoparticles.

Preparation of $Co_3O_4@SiO_2$ nanocomposites under ultrasound irradiation

The $Co_3O_4@SiO_2$ nanocomposites were prepared according to the previously reported method by Vela et al. with some minor modifications (28). Briefly, CTAB (2.2 g) was added to a solution of Co_3O_4 nanocomposites (0.5 g) in EtOH (350 mL), and then concentrated ammonia aqueous solution (40 mL, 28 wt %) was added dropwise to the reaction mixture for 20 min under sonication. Afterwards, tetraethylorthosilicate (TEOS) (0.4 mL in 10 mL of EtOH) was added to the mixture under ultrasound irradiation. The solution was stirred for 20 h at room temperature. The prepared silica-coated cobalt oxide nanocomposite was collected by centrifugation, washed three times with deionized water, and then calcined at 600°C for 6 h.

Typical procedure for the synthesis of 2-pyrrolidinon-3-olate derivatives

In a two-necked flask, a solution of dimethyl acetylenedicarboxylate (1 mmol) and morpholine/piperidine (1 mmol) in ethanol (3 mL) and water (3 mL) was sonicated (40 kHz frequency and 80 W powers) for 10 min at room temperature. Then 2-aminobenzothiazole (1 mmol), aromatic aldehyde (1 mmol) and the $Co_3O_4@SiO_2$ nanocomposites (0.003 g) were added and sonicated for the appropriate time (monitored by TLC). After completion of the reaction, the mixture was cooled down to room temperature and then was centrifuged to separate the catalyst. The solvent was evaporated under

vacuum and the solid obtained was recrystallized from EtOH to give the pure 2-pyrrolidinon-3-olates.

Spectral data of products

Morpholin-4-ium-1-(benzo[d]thiazol-2-yl)-5-(4-nitrophenyl)-4-(methoxycarbonyl)-2-oxo-2,5-dihydro-1H-pyrrol-3-olate (5h)

White solid, m.p 198–199°C. ^1H NMR (400 MHz, DMSO-d_6) δ: 2.08 (s, 4 H, 2 × CH_2), 2.41 (s, 3 H, CH_3), 3.85 (s, 4 H, 2 × CH_2), 6.04 (s, 1 H, CH), 6.92–7.50 (m, 8 H, ArH), 9.14 (s, 2 H, NH); ^{13}C NMR (100 MHz, DMSO-d_6) δ: 25.1, 51.8, 58.6, 62.5 104.2, 121.1, 121.9, 123.9, 124.1, 126.3 128.6, 129.2, 134.7, 135.5, 146.8 147.0, 159.4, 164.2, 165.1; IR (KBr) v: 3402, 2970, 1710, 1447, cm^{-1}; MS (EI) (m/z): 498.12 (M$^+$); Anal. Calcd for $C_{23}H_{22}N_4O_7S$: C 55.42, H 4.45, N 11.24. Found: C 55.56, H 4.38, N 11.21.

Morpholin-4-ium-1-(benzo[d]thiazol-2-yl)-5-(4-chlorophenyl)-4-(methoxycarbonyl)-2-oxo-2,5-dihydro-1H-pyrrol-3-olate (5i)

White solid, m.p 192–194°C. ^1H NMR (400 MHz, DMSO-d_6) δ : 2.40 (s, 4 H, 2 × CH_2), 2.65 (s, 3 H, CH_3), 3.98 (s, 4 H, 2 × CH_2), 6.02 (s, 1 H, CH), 6.72–7.30 (m, 8 H, ArH), 9.49 (s, 2 H, NH); ^{13}C NMR (100 MHz, DMSO-d_6) δ : 28.4, 36.7, 48.5, 52.4, 110.7, 112.6, 114.7, 116.2, 118.3, 118.9, 124.8, 129.7, 131.2, 132.3, 139.6, 144.5, 147.2, 156.8, 160.2, 164.9; IR (KBr) v: 3420, 2965, 1715, 1448, cm^{-1}; MS (EI) (m/z): 487.10 (M$^+$); Anal. Calcd for $C_{23}H_{22}ClN_3O_5S$: C 56.61, H 4.54, N 8.61. Found: C 56.58, H 4.59, N 8.73.

Morpholin-4-ium-1-(benzo[d]thiazol-2-yl)-5-(4-bromophenyl)-4-(methoxycarbonyl)-2-oxo-2,5-dihydro-1H-pyrrol-3-olate (5j)

White solid, m.p 176–178°C. ^1H NMR (400 MHz, DMSO-d_6) δ : 2.82 (s, 4 H, 2 × CH_2), 3.41 (s, 3 H, CH_3), 3.88 (s, 4 H, 2 × CH_2), 5.95 (s, 1 H, CH), 6.92–7.73 (m, 8 H, ArH), 9.91 (s, 2 H, NH); ^{13}C NMR (100 MHz, DMSO-d_6) δ : 27.2, 28.3, 46.3, 49.8, 112.3, 115.1, 118.1, 120.8, 121.5, 123.8, 126.0, 129.6, 130.0, 130.8, 131.1, 137.2, 143.3, 150.4, 165.0; IR (KBr) v: 3390, 2058, 1700, 1448, cm^{-1}; MS (EI) (m/z): 531.05 (M$^+$); Anal. Calcd for $C_{23}H_{22}BrN_3O_5S$: C 51.89, H 4.17, N 7.89. Found: C 51.80, H 4.23, N 7.96.

Morpholin-4-ium-1-(benzo[d]thiazol-2-yl)-5-(4-hydroxyphenyl)-4-(methoxycarbonyl)-2-oxo-2,5-dihydro-1H-pyrrol-3-olate (5k)

White solid, m.p 209–211°C. ^1H NMR (400 MHz, DMSO-d_6) δ : 2.28 (s, 4 H, 2 × CH_2), 3.50 (s, 3 H, CH_3), 3.94 (s, 4 H, 2 × CH_2), 6.05 (s, 1 H, CH), 6.45–7.29 (m, 8 H, ArH), 8.86 (s, 1H, OH), 9.65 (s, 2 H, NH); ^{13}C NMR (100 MHz, DMSO-d_6) δ : 20.0, 33.5, 40.8, 54.6, 112.2, 115.4, 116.1, 117.2, 126.0, 128.4, 129.6, 131.3, 135.5, 143.8, 152.7, 157.4, 164.2, 165.8; IR (KBr) v: 3650, 3370, 2940, 1705,
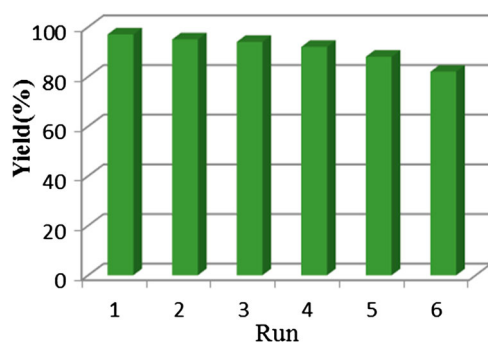
Figure 7. Reusability of the $Co_3O_4@SiO_2$ nanostructures.

1441, cm^{-1}; MS (EI) (m/z): 469.13 (M^+); Anal. Calcd for $C_{23}H_{23}N_3O_6S$: C 58.84, H 4.94, N 8.95. Found: C 58.89, H 4.91, N 8.88.

Recycling and reusing of the catalyst

In order to investigate the reusability of the catalyst, the model reaction was repeated using recovered $Co_3O_4@SiO_2$ core–shell nanocomposite under the optimized reaction conditions. Upon completion of the reaction, the catalyst was separated by an external magnet then washed with dichloromethane and ethyl acetate, and the recycled catalyst was saved for the next reaction. We observed that the recovered nanocomposites could be used for six successive runs with a slightly decreased activity, as shown in Figure 7.

Conclusions

In summary, we have developed an effective route for the synthesis of 2-pyrrolidinon-3-olate derivatives using various aryl aldehyde, 2-aminobenzothiazole, dimethyl acetylenedicarboxylate and morpholine/piperidine in the presence of $Co_3O_4@SiO_2$ nanocomposites under ultrasonic irradiation. The synergistic effect of ultrasound has been successfully demonstrated to offer an environment-friendly method for the synthesis of 2-pyrrolidinon-3-olates with excellent yields and short reaction times.

Disclosure statement

No potential conflict of interest was reported by the authors.

Funding

Notes on contributors

Mohammad Ali Ghasemzadeh received B.S., M.S. and Ph.D. degrees in Chemistry and Organic Chemistry from the University of Kashan, Iran, in 2005, 2008 and 2012, respectively. He is currently assistant professor in the Department of Chemistry, Qom Branch, Islamic Azad University. His research interests lie in multi-component reactions, nanoscience and nanotechnology, application of functionalized metal nanostructures as catalyst in the organic transformations and also ionic liquids in organic synthesis.

Mohammad Hossein Abdollahi-Basir received a B.S. degree in Applied Chemistry from the Qom Branch, Islamic Azad University, Iran, in 2012, a M.S. degree in Organic Chemistry from Yadegar-e-Imam Khomeini (RAH) Branch, Islamic Azad University, Iran, in 2014, and is now a Ph.D. student in Organic Chemistry at QomBranch, Islamic Azad University, Iran. His research interests lie in core-shell nanostructures, application of nanocatalysts (synthesis and characterization) and using of them in multi-component reactions.

References

(1) Gnanasambandam, V.; Kandhasamy, K. *Tetrahedron Lett.* **2008**, *39*, 5636–5638.
(2) Dabholkara, V.V.; Ansaria, F.Y. *Green. Chem. Lett. Rev.* **2010**, *3*, 245–248.
(3) Ruiz, E.; Rodriguez, H.; Coro, J.; Salfran, E.; Suarez, M.; Alvarez, R.M.; Martin, N. *Ultrason. Sonochem.* **2011**, *18*, 32–36.
(4) Pagadala, R.; Maddilaa, S.; Jonnalagadda, S.B. *Green. Chem. Lett. Rev.* **2014**, *7*, 131–136.
(5) Singh, A.K.; Shukla, S.K.; Quraishi, M.A. *J. Mater. Environ. Sci.* **2011**, *2*, 403–406.
(6) Xu, H.; Liao, W.M.; Li, H.F. *Ultrason. Sonochem.* **2007**, *14*, 779–782.
(7) Winbal, B. *CNS Drug Rev.* **2005**, *11*, 169–182.
(8) Siddiqui, N.; Ahsan, W.; Alam, M.S.; Ali, R.; Srivastava, K. *Arch. Pharm. Chem. Life Sci.* **2012**, *345*, 185–194.
(9) Volkhard, A.; Eisert, W.; Himmelsbach, F.; Linz, G.; Mueller, T.; Pieper, H.; Weisenberger, J. US Patent 5455348, November 3, **1995**.
(10) Zhongli, G.; Ryan, H.; David, S. US Patent 20120238757, September 20, **2012**.
(11) (a) Cornlis, B.; Herrmann, W.A.; Muhler, M.; Wong, C.H. *Catalysis from A to Z: A Concise Encyclopedia*. Wiley-VCH: Weinheim, **2007**, 1–3; (b) Sheldon, R.; Arends, L.; Hanefeld, U. *Green Chemistry and Catalysis*. Wiley-VCH: Weinheim, **2007**.
(12) (a) Lee, S.H.; Park, D.R.; Kim, H.; Lee, J.H.; Jung, J.C.; Woo, S.Y.; Song, W.S.; Kwon, M.S.; Song, I.K. *Catal Commun.* **2008**, *9*, 1920–1923; (b) Park, S.; Cho, K.M.; Youn, M.H.; Seo, J.G.; Baeck, S.H.; Kim, T.J.; Chung, Y.M.; Oh, S.; Song, I.K. *Catal Lett.* **2008**, *122*, 349–353.
(13) Beydoun, D.; Amal, R.; Low, G.; McEvoy, S. *J. Mol. Catal. A-Chem.* **2002**, *180*, 193–200.
(14) Girgis, E.; Wahsh, M.M.; Othman, A.J.; Bandhu, L.; Rao, K.V. *Nano. Res. Lett.* **2011**, *6*, 460–466.
(15) Maleki, A. *Tetrahedron Lett.* **2013**, *54*, 2055–2059.
(16) Kiasat, A.R.; Davarpanah, J. *J. Mol. Catal. A-Chem.* **2013**, *373*, 46–54.

(17) Zamani, F.; Izadi, E. *Catal. Commun.* **2013**, *42*, 104–108.

(18) Naeimi, H.; Nazifi, Z.S. *J. Nanopart. Res.* **2013**, *15*, 2026–2037.

(19) Esmaeilpour, M.; Sardarian, A.R. *Green. Chem. Lett. Rev.* **2014**, *7*, 301–308.

(20) Li, B.; Zhang, M.; Hu, H.; Du, X.; Zhang, Z. *New. J. Chem.* **2014**, *38*, 2435–2442.

(21) Gao, H.; Sun, J.; Yan, C.G. *Beilstein J. Org. Chem.* **2013**, *9*, 2934–2939.

(22) Ghasemzadeh, M.A.; Safaei-Ghomi, J.; Molaei, H.C.R. *Chimie.* **2012**, *15*, 969–974.

(23) Ghasemzadeh, M.A.; Ghasemi-Seresht, N. *Res. Chem. Intermed.* **2015**, *41*, 8625–8636.

(24) Ghasemzadeh, M.A.; Safaei-Ghomi, J.; Zahedi, S. *J. Serb. Chem. Soc.* **2013**, *78*, 769–779.

(25) Ghasemzadeh, M.A.; Abdollahi-Basir, M.H.; Babaei, M. *Green. Chem. Lett. Rev.* **2015**, *8*, 40–49.

(26) Safaei-Ghomi, J.; Ghasemzadeh, M.A. *J. Serb. Chem. Soc.* **2011**, *76*, 679–684.

(27) Suryanarayana, C.; Norton, M.G. *X-Ray Diffraction: A Practical Approach*; Plenum Press: New York, **1998**.

(28) Lin, C. C.; Guo, Y.; Vela, J. *ACS Catal.* **2015**, *5*, 1037–1044.